Research Square

Preprints are preliminary reports that have not undergone peer review.
They should not be considered conclusive, used to inform clinical practice,
or referenced by the media as validated information.

A prospective high-resolution ultrasonography and 3 Tesla MR imaging correlation in patients with chronic shoulder pain in a tertiary care centre of eastern India

Nitish Upadhyay

nirajk409@gmail.com

Institute of Post Graduate Medical Education and Research

Sohini Sengupta

North Bengal Medical College and Hospital

Ananda Kisor Pal

Institute of Post Graduate Medical Education and Research

Research Article

Keywords: Rotator cuff, High-resolution ultrasonography, Magnetic resonance imaging, Shoulder pain, Tendon tear, Tendinosis

Posted Date: June 24th, 2026

DOI: https://doi.org/10.21203/rs.3.rs-9215431/v1

License: This work is licensed under a Creative Commons Attribution 4.0 International License.
Read Full License

Additional Declarations: No competing interests reported.

Abstract

Background

Shoulder pain is one of the most prevalent musculoskeletal complaints encountered in orthopaedic practice. Rotator cuff disorders represent the most common cause. High-resolution ultrasonography (HRUSG) is a readily available, cost-effective, dynamic imaging modality, while 3 Tesla (3T) MRI is widely regarded as the reference standard. This prospective study aimed to evaluate the diagnostic accuracy of HRUSG in detecting rotator cuff tendon pathologies and to correlate its findings with 3T MRI.

Methods

Fifty-nine patients with chronic shoulder pain (duration ≥ 6 months) and clinical suspicion of rotator cuff pathology were prospectively enrolled between March 2021 and August 2022 at a tertiary care centre in eastern India. All patients underwent HRUSG followed by 3T MRI of the affected shoulder. Findings were classified as full-thickness tear, partial-thickness tear, intrasubstance tear, tendinosis, or normal for each tendon. Diagnostic accuracy indices and kappa agreement statistics were calculated.

Results

The study population comprised 59 patients (mean age range 26–65 years; 56% male). The supraspinatus was the most commonly affected tendon. For full-thickness tears, HRUSG demonstrated sensitivity of 100%, specificity of 92.31%, positive predictive value (PPV) of 86.96%, negative predictive value (NPV) of 100%, and overall accuracy of 94.92%. For partial-thickness tears: sensitivity 93.55%, specificity 78.57%, PPV 82.86%, NPV 91.67%, and accuracy 86.44%. For tendinosis: sensitivity 86.36%, specificity 80.00%, PPV 92.68%, NPV 66.67%, and accuracy 84.25%. Kappa agreement was ‘almost perfect’ for full-thickness tears (k = 0.89) and tendinosis (k = 0.85), and ‘substantial’ for partial-thickness tears (k = 0.72).

Conclusions

HRUSG shows high sensitivity and specificity for detecting rotator cuff tears and compares favourably with 3T MRI. It can serve as a reliable first-line imaging modality for chronic shoulder pain. MRI should be reserved as a problem-solving tool, particularly for labral and capsular pathologies and pre-surgical planning.

Background

Shoulder pain is the third most prevalent reason for attendance at an orthopaedic clinic [1]. Common causes include tendon inflammation, tendon tears, joint instability, arthritis, and fractures. Rotator cuff disorders represent the most frequent cause of painful shoulder [2]. The rotator cuff tendons are

vulnerable to degeneration due to constant active and passive mechanical forces, resulting in tendon swelling and subluxation [3].

Ultrasonography (USG) and magnetic resonance imaging (MRI) are the two most widely used modalities for evaluating shoulder pathologies. The shoulder joint is the most common site for musculoskeletal USG evaluation [4]. USG offers an easy, inexpensive, quick, non-invasive assessment of rotator cuff and non-rotator cuff abnormalities [5, 6]. It permits dynamic examination in multiple planes and allows rapid targeting of areas of concern. However, its limitations include significant operator dependence, restricted evaluation of labral lesions and the rotator cuff interval, an inability to detect subtle bone lesions, and inter-observer variability.

MRI, with its excellent contrast resolution, enables a thorough non-invasive assessment of soft tissues. It provides detailed information about rotator cuff pathology including tear size, extent of retraction, and degree of muscle atrophy, facilitating surgical planning [7]. MRI also detects ganglion cysts, labral injuries, and biceps tendon abnormalities. Despite being the reference standard, MRI is costly, time-consuming, less universally accessible, and contraindicated in patients with pacemakers, cochlear implants, or claustrophobia.

High-resolution USG (HRUSG) has seen increasing application in sports medicine and musculoskeletal radiology over recent decades [35]. Its widespread availability and growing use have prompted investigators to determine its diagnostic accuracy against MRI for rotator cuff lesions. Published studies have produced variable results, particularly in elderly patients with chronic degenerative conditions. A recent meta-analysis suggested MRI had the highest sensitivity and specificity for diagnosing full- and partial-thickness rotator cuff tears. This study was therefore designed to prospectively compare HRUSG findings with 3T MRI in patients presenting with chronic shoulder pain at a tertiary care centre in eastern India.

Methods

Study design and setting

This was an institution-based, prospective, observational cross-sectional diagnostic accuracy study conducted in the Department of Radiodiagnosis at a tertiary care teaching hospital in eastern India, between March 2021 and August 2022 (18 months including preparatory, data collection, analysis, and writing phases).

Ethical approval

The study was approved by the Institutional Ethics Committee (IEC) of the study institution (IEC approval reference withheld for blind review). Written informed consent was obtained from all participants prior to enrolment. The study was conducted in accordance with the Declaration of Helsinki.

Participants

Patients of either sex referred from the Department of Orthopaedics with shoulder pain and restricted shoulder movement were prospectively enrolled. Inclusion criteria were: (1) history of pain in either shoulder; (2) history of restricted range of motion; (3) clinical suspicion of rotator cuff tear with symptom duration of at least 6 months. Exclusion criteria were: (1) contraindication to MRI; (2) known fracture or dislocation on plain radiography; (3) previous shoulder surgery.

A minimum sample size of 50 (±10) was determined by convenience sampling based on an estimated 3–5 eligible referrals per week during the data collection period.

Imaging protocols

High-Resolution Ultrasonography (HRUSG)

HRUSG was performed using a GE LOGIQ P9 machine with a high-frequency linear array probe (3–12 MHz). Patients were seated on a rotating stool, allowing examination of all shoulder regions. Standard examination included: (1) anterior region – long head of biceps tendon (LHBT) and subscapularis with the arm in slight internal rotation and elbow flexed at 90°; (2) anterolateral region – supraspinatus with the patient's palm placed on the ipsilateral iliac wing (modified Crass position); (3) posterior region – infraspinatus and teres minor with the transducer over the posterior glenohumeral joint. All tendons were evaluated in both longitudinal and transverse planes to avoid anisotropy artefact.

3 Tesla MRI

MRI was performed on a GE Signa HDxt 3T machine using a dedicated shoulder coil. The patient lay supine with the arm in neutral position, thumb pointing upward. Multiplanar images were acquired in axial, oblique coronal, and oblique sagittal planes. Sequences included: Coronal PD (TR 4500/TE 32/slice 2.0 mm/FOV 140×140/matrix 320×75), Coronal T2 FS (TR 3500/TE 72/slice 3.0 mm), Sagittal T1 (TR 600/TE 11/slice 2.5 mm), Sagittal T2 FS (TR 5000/TE 62/slice 2.5 mm), and Axial PD (TR 3030/TE 33/slice 2.0 mm/FOV 140×140/matrix 256×100).

Diagnostic criteria

USG diagnostic criteria: full-thickness tear – focal or complete non-visualisation of the tendon, or an anechoic defect extending from the bursal to the articular surface; partial-thickness tear – anechoic or hypoechoic defect extending to either the bursal or articular surface without through-and-through involvement; intrasubstance tear – intratendinous fluid-filled longitudinal split not exiting either surface; tendinosis – tendon thickening and/or hypoechoic appearance with effacement of the fibrillar pattern.

MRI diagnostic criteria: full-thickness tear – tendon defect extending from articular to bursal surface filled with fluid signal on T2-weighted sequences; partial-thickness tear – focal region of fibre discontinuity with fluid signal not extending the full thickness; intrasubstance tear – intratendinous T2 hyperintensity not reaching either surface; tendinosis – increased signal on proton density sequences without corresponding T2 fluid signal (magic angle artefact excluded by comparison with long-TE sequences).

Statistical analysis

HRUSG findings were compared with 3T MRI (reference standard) to calculate sensitivity, specificity, positive predictive value (PPV), negative predictive value (NPV), and overall accuracy for each pathological category. Inter-modality agreement was assessed using the weighted kappa statistic (k). Kappa values were interpreted as: 0.21–0.40 = fair; 0.41–0.60 = moderate; 0.61–0.80 = substantial; >0.81 = almost perfect agreement (Landis and Koch criteria).

Results

Demographics and clinical characteristics

Fifty-nine patients with chronic shoulder pain were enrolled (age range 26–65 years). The majority (37.3%) were aged ≤40 years, followed by 33.9% in the 41–50 year group, and 28.8% aged >50 years. Males comprised 55.9% (n=33) and females 44.1% (n=26). Right shoulder involvement was more frequent (61.0%, n=36) than left (39.0%, n=23). Most patients (77.97%, n=46) presented between 6 and 9 months after symptom onset. A history of trauma was recalled by 44.1% (n=26). Comorbidities included diabetes mellitus (25.4%, n=15) and rheumatoid arthritis (6.8%, n=4); 67.8% (n=40) had no comorbidity.

Table 1 summarises the demographic and clinical profile.

Variable	Category	n	%
Age group	≤40 years	22	37.3%
	41–50 years	20	33.9%
	>50 years	17	28.8%
Sex	Male	33	55.9%
	Female	26	44.1%
Laterality	Right shoulder	36	61.0%
	Left shoulder	23	39.0%
Duration	6–9 months	46	78.0%
	>9 months	13	22.0%
Trauma history	Yes	26	44.1%
	No	33	55.9%
Comorbidity	Diabetes mellitus	15	25.4%
	Rheumatoid arthritis	4	6.8%
	None	40	67.8%

Table 1. Demographic and clinical characteristics of the study population (n=59).

Imaging findings by tendon

Table 2 provides a detailed comparison of HRUSG and 3T MRI findings for all rotator cuff tendons.

Tendon	Pathology	USG n (%)	MRI n (%)
Subscapularis	Full-thickness tear	10 (16.9%)	8 (13.6%)
	Partial-thickness tear	16 (27.1%)	12 (20.3%)
	Intrasubstance tear	3 (5.1%)	3 (5.1%)
	Tendinosis	18 (30.5%)	15 (25.4%)
	Normal	12 (20.3%)	21 (35.6%)
Supraspinatus	Full-thickness tear	10 (16.9%)	9 (15.3%)
	Partial-thickness tear	13 (22.0%)	15 (25.4%)
	Intrasubstance tear	5 (8.5%)	8 (13.6%)
	Tendinosis	7 (11.9%)	9 (15.3%)
	Normal	24 (40.7%)	18 (30.5%)
Infraspinatus	Full-thickness tear	1 (1.7%)	1 (1.7%)
	Partial-thickness tear	0 (0%)	0 (0%)
	Intrasubstance tear	0 (0%)	1 (1.7%)
	Tendinosis	1 (1.7%)	3 (5.1%)
	Normal	57 (96.6%)	54 (91.5%)
LHBT	Full-thickness tear	2 (3.4%)	2 (3.4%)
	Partial-thickness tear	4 (6.8%)	2 (3.4%)
	Intrasubstance tear	0 (0%)	0 (0%)
	Tendinosis	9 (15.3%)	11 (18.6%)
	Normal	44 (74.6%)	44 (74.6%)
Teres minor	All categories	Normal (0%)	Normal (0%)

Table 2. Comparative distribution of pathologies on HRUSG and 3T MRI for all rotator cuff tendons (n=59). LHBT = long head of biceps tendon.

Diagnostic accuracy of HRUSG

Table 3 summarises the overall diagnostic performance of HRUSG across all pathological categories using 3T MRI as the reference standard.

Pathology	TP	FP	TN	FN	Sensitivity	Specificity	PPV	NPV	Accuracy
Full-thickness tear	20	3	36	0	100%	92.31%	86.96%	100%	94.92%
Partial-thickness tear	29	6	22	2	93.55%	78.57%	82.86%	91.67%	86.44%
Tendinosis	38	3	12	6	86.36%	80.00%	92.68%	66.67%	84.25%
Intrasubstance tear	12	0	43	4	75.00%	100%	100%	91.49%	93.22%

Table 3. Overall diagnostic accuracy of HRUSG for rotator cuff pathologies (MRI as reference standard). TP = true positive; FP = false positive; TN = true negative; FN = false negative; PPV = positive predictive value; NPV = negative predictive value.

Inter-modality agreement (kappa statistics)

Table 4 presents weighted kappa values for agreement between HRUSG and 3T MRI.

Pathological finding	Kappa (k)	Interpretation
Full-thickness tear	0.89	Almost perfect
Tendinosis	0.85	Almost perfect
Partial-thickness tear	0.72	Substantial
Intrasubstance tear	0.40	Fair

Table 4. Weighted kappa agreement between HRUSG and 3T MRI for rotator cuff pathologies.

Discussion

This prospective cross-sectional study evaluated the diagnostic accuracy of HRUSG against 3T MRI for rotator cuff tendon pathologies in 59 patients with chronic shoulder pain at a tertiary care centre in eastern India. The key finding was that HRUSG demonstrated excellent sensitivity and specificity for full-thickness tears (100% and 92.31%, respectively) with almost perfect kappa agreement (k=0.89), and high sensitivity for partial-thickness tears (93.55%) with substantial agreement (k=0.72), supporting its role as a reliable first-line imaging modality.

The demographic profile of our study differed slightly from some Western series. Singh et al. [12] reported predominance in the 56–65 year age group, whereas in our cohort the majority (37%) were aged under 40, possibly reflecting the younger, more physically active population presenting to our tertiary orthopaedic service and a higher prevalence of traumatic rather than purely degenerative pathology. The male predominance (56%) and right shoulder preponderance (61%) are consistent with dominant-limb overuse

being an important aetiological factor, in agreement with Elaassar et al. [24] who reported 72% right-hand dominance in their series.

The supraspinatus tendon was the most frequently affected structure on both modalities (69.5% on MRI), consistent with its anatomical position between the greater tuberosity and the acromion, subjecting it to repeated impingement during overhead activity – a finding corroborated by Zlatkin et al. [29] who reported supraspinatus involvement in approximately 80% of cases. Partial-thickness tear was the most common supraspinatus pathology, while tendinosis predominated in the subscapularis and LHBT. No teres minor pathology was identified in this series.

The diagnostic accuracy for full-thickness tears in our study (sensitivity 100%, specificity 92.31%, accuracy 94.92%) is comparable to findings reported by Bashir et al. [31] and Fischer et al. [9] (accuracy 91.1% for supraspinatus). Our results also accord with Cullen et al. [33] who found sensitivity of 89% and specificity of 100% for full-thickness tears, and El-Shewi et al. [18] who demonstrated sensitivity of 90% for full-thickness tears on dynamic USG. For partial-thickness tears, our sensitivity of 93.55% and specificity of 78.57% compare favourably with those of Singh AP et al. [13] (sensitivity 78.04%, specificity 89.47%) and Netam et al. [14] (sensitivity 92.9%, specificity 86%).

The relatively lower accuracy for intrasubstance tears (kappa 0.40, fair agreement) reflects the inherent limitation of HRUSG in detecting intratendinous pathology that does not breach either the articular or bursal surface, a finding consistent with the literature. Similarly, the lower NPV for tendinosis (66.67%) indicates that HRUSG can miss mild tendinopathic changes better appreciated on MRI proton density sequences.

MRI demonstrated superior sensitivity for intrasubstance tears and tendinosis, and retains its unique advantage for evaluating labral pathologies, glenohumeral ligaments, and bone marrow changes, which are inaccessible to USG. Consistent with Wengert et al. [17] and Narra et al. [11], our findings support a complementary role for the two modalities: HRUSG as the initial cost-effective dynamic screening tool, with MRI reserved for cases with diagnostic uncertainty or where surgical planning requires comprehensive joint assessment.

Limitations of this study include the relatively small sample size, the lack of arthroscopic correlation as the ultimate reference standard, operator dependence of HRUSG, and the absence of MR arthrography which would have allowed more precise labral evaluation. Future multicentre studies with surgical correlation are warranted.

Conclusion

HRUSG demonstrates high sensitivity and specificity for full-thickness and partial-thickness rotator cuff tears when compared with 3T MRI, with almost perfect agreement for full-thickness tears. It can reliably serve as the first-line imaging modality for evaluating chronic shoulder pain given its wide availability, lower cost, and patient tolerance. MRI should be reserved as a complementary problem-solving tool,

particularly where labral or capsular pathologies are suspected or surgical intervention is planned. Further improvement in HRUSG diagnostic accuracy is expected with increasing operator experience and technologic advances.

Abbreviations

HRUSG
High-resolution ultrasonography
MRI
Magnetic resonance imaging
3T
3 Tesla
LHBT
Long head of biceps tendon
PPV
Positive predictive value
NPV
Negative predictive value
TP
True positive
FP
False positive
TN
True negative
FN
False negative
PDFS
Proton density fat suppressed
IEC
Institutional Ethics Committee

Declarations

Ethics approval and consent to participate: The study was approved by the Institutional Ethics Committee of the study institution (IEC approval reference withheld for blind review). Written informed consent was obtained from all participants before enrolment. All procedures were performed in accordance with the Declaration of Helsinki.

Consent for publication: Written informed consent for publication of anonymised clinical and imaging data was obtained from all participating patients. No individually identifiable data are included in this manuscript.

Availability of data and materials: The dataset supporting the conclusions of this article is included within the article and its additional file (Additional file 1: Master chart of patient data and imaging findings).

Competing interests: The authors declare that they have no competing interests.

Funding: No specific funding was received for this study.

Acknowledgements: [Acknowledgements withheld for double-blind peer review. Will be restored upon acceptance.]

References

1. Dinnes J, Loveman E, McIntyre L, Waugh N. The effectiveness of diagnostic tests for the assessment of shoulder pain due to soft tissue disorders: a systematic review. Health Technol Assess. 2003;7(29):iii,1–166.
2. Uhthoff HK, Sarkar K. An algorithm for shoulder pain caused by soft-tissue disorders. Clin Orthop Relat Res. 1990;(254):121–27.
3. Lambert A, Loffroy R, Guiu B, Mejean N, Lerais JM, Cercueil JP, et al. Rotator cuff tears: value of 3.0T MRI. J Radiol. 2009;90(5 Pt 1):583–88.
4. Chaubal NG. Ultrasonography of shoulder (rotator cuff). Indian J Radiol Imaging. 2007;17:209–14.
5. Seibold CJ, Mallisee TA, Erickson SJ, Boynton MD, Raasch WG, Timins ME. Rotator cuff: evaluation with US and MR imaging. Radiographics. 1999;19(3):685–705.
6. Martinoli C, Bianchi S, Prato N, Pugliese F, Zamorani MP, Valle M, et al. US of the shoulder: non-rotator cuff disorders. Radiographics. 2003;23(2):381–401.
7. Sher JS, Iannotti JP, Williams GR, Herzog RJ, Kneeland JB, Lisser S, et al. The effect of shoulder MRI on clinical decision making. J Shoulder Elbow Surg. 1998;7(3):205–09.
8. Jung JY, Jee WH, Chun HJ, Ahn MI, Kim YS. Magnetic resonance arthrography including ABER view in diagnosing partial-thickness tears of the rotator cuff. Acta Radiol. 2010;51(2):194–201.
9. Fischer CA, Weber MA, Neubecker C, Bruckner T, Tanner M, Zeifang F. Ultrasound vs. MRI in the assessment of rotator cuff structure prior to shoulder arthroplasty. J Orthop. 2015;12(1):23–30.
10. Lee MH, Sheehan SE, Orwin JF, Lee KS. Comprehensive shoulder US examination: a standardized approach with multimodality correlation for common shoulder disease. Radiographics. 2016;36(6):1606.
11. Narra R, Jehendren VM, Bollipo JP, Putcha A. Sonographic evaluation of shoulder joint pain with MRI correlation. J Evol Med Dent Sci. 2017;6(37):3007–14.
12. Singh A, Thukral CL, Gupta K, Singh MI, Lata S, Arora RK. Role and correlation of high resolution ultrasound and magnetic resonance imaging in evaluation of patients with shoulder pain. Pol J Radiol. 2017;82:410–7.
13. Singh AP, Rao A, Devaru S, Amithavikrama S. Role of ultrasound in evaluation of shoulder injuries: a comparative study with MRI. Int J Anat Radiol Surg. 2017;6(1):R012–R8.

14. Netam SB, Kumar S, Jain V, Singh A, Singh RK. Role of ultrasonography in evaluation of rotator cuff in patients of chronic shoulder pain in comparison to MRI. Int J Sci Study. 2017;5(3):291–6.
15. Park J, Chai JW, Kim DH, Cha SW. Dynamic ultrasonography of the shoulder. Ultrasonography. 2018;37(3):190.
16. Naganna HP, Rangaswamy SM, Jaganathan NC, Lingaiah RK, Nagarajegowda PH. Study of rotator cuff disorders by ultrasound with MRI correlation. 2018.
17. Wengert GJ, Schmutzer M, Bickel H, Sora MC, Polanec SH, Weber M, et al. Reliability of high-resolution ultrasound and MR arthrography of the shoulder in patients with sports-related shoulder injuries. PLoS One. 2019;14(9):e0222783.
18. El-Shewi IE, El Azizy HM, Gadalla AA. Role of dynamic ultrasound versus MRI in diagnosis and assessment of shoulder impingement syndrome. Egypt J Radiol Nucl Med. 2019;50(1):1–7.
19. Frere RA, Libda I, Tantawy F, Sakr HM, El-Alfy AT. Sonoelastography, conventional ultrasound and MRI in detection of rotator cuff lesions in patients with chronic shoulder pain. Egypt Rheumatol. 2021;43(1):17–21.
20. Singh P, Kaur A, Bhagat S, Singh GB, Gupta N. Role of ultrasound and MRI in patients with shoulder pathologies: a correlation study. Eur J Mol Clin Med. 2021;8(03).
21. Barad HV, Patel V, Patel S, Patel M. To determine the role of ultrasonography as a primary imaging modality as compared to MRI in patients with shoulder pain. J Fam Med Prim Care. 2022;11(5):2119–22.
22. Naqvi GA, Jadaan M, Harrington P. Accuracy of ultrasonography and MRI for detection of full thickness rotator cuff tears. Int J Shoulder Surg. 2009;3(4):94–97.
23. Elaassar MMN, Emadeldin A, Zidan DZ, Sakr HM, Abdelazim H. Chronic non-traumatic shoulder pain: evaluation with ultrasonography and conventional MR imaging. QJM. 2020;113(Suppl_1):hcaa068.013.
24. Thomas SJ, McDougall C, Brown IDM, Jaberoo MC, Stearns A, Ashraf R, et al. Prevalence of symptoms and signs of shoulder problems in people with diabetes mellitus. J Shoulder Elbow Surg. 2007;16(6):748–51.
25. Chen DY, Lan HHC, Lai KL, Chen HH, Chen YM, Chen CP. Diagnostic utility of US for detecting rotator cuff tears in rheumatoid arthritis patients: comparison with MRI. J Med Ultrasound. 2014;22(4):200–6.
26. Kim HA, Kim SH, Seo YI. Ultrasonographic findings of the shoulder in patients with rheumatoid arthritis and comparison with physical examination. J Korean Med Sci. 2007;22(4):660–6.
27. Zlatkin MB, Reicher MA, Kellerhouse LE, McDade W, Vetter L, Resnick D, et al. The painful shoulder: MR imaging of the glenohumeral joint. J Comput Assist Tomogr. 1988;12:995–1001.
28. Mitchell C, Adebajo A, Hay E, Carr A. Shoulder pain: diagnosis and management in primary care. BMJ. 2005;331(7525):1124–28.
29. Bashir S, Firdose SR, Kamal Y, Khan HA, Arora M, Gul S, et al. Correlation between high resolution ultrasonography and MRI in rotator cuff tear diagnosis. IJHSR. 2014;4(8):103–12.

30. Rutten MJ, Spaargaren GJ, van Loon T, de Waal Malefijt MC, Kiemeney LA, Jager GJ. Detection of rotator cuff tears: the value of MRI following ultrasound. Eur Radiol. 2010;20(2):450–57.
31. Cullen DM, Breidahl WH, Janes GC. Diagnostic accuracy of shoulder ultrasound performed by a single operator. Australas Radiol. 2007;51(3):226–29.
32. Coris EE, Pescasio M, Zwygart K, Gonzalez E, Farrar T, Bryan S, et al. Office-based ultrasound in sports medicine practice. Clin J Sport Med. 2011;21(1):57–61.
33. Farin PU, Jaroma H, Harju A, Soimakallio S. Shoulder impingement syndrome: sonographic evaluation. Radiology. 1990;176(3):845–49.
34. Zlatkin MB. Rotator Cuff Disease. In: Zlatkin MB. MRI of the Shoulder. 2nd ed. Philadelphia: Lippincott Williams & Wilkins; 2003.
35. Jacobson JA. Shoulder US: anatomy, technique, and scanning pitfalls. Radiology. 2011;260(1):6–16.
36. Levine BD, Motamedi K, Seeger LL. Imaging of the shoulder: a comparison of MRI and ultrasound. Curr Sports Med Rep. 2012;11(5):239–43.

Figures



Figure 1

Imaging equipment used in the study

A *GE Healthcare Signa HDxt 3 Tesla MRI machine used for all MRI examinations.* **B** *Dedicated shoulder surface coil used during 3T MRI acquisition.* **C** *GE Healthcare LOGIQ P9 ultrasound machine employed for all HRUSG examinations.* **D** *High-frequency linear array transducer (3–12 MHz) used for rotator cuff evaluation. HRUSG = high-resolution ultrasonography; MRI = magnetic resonance imaging.*

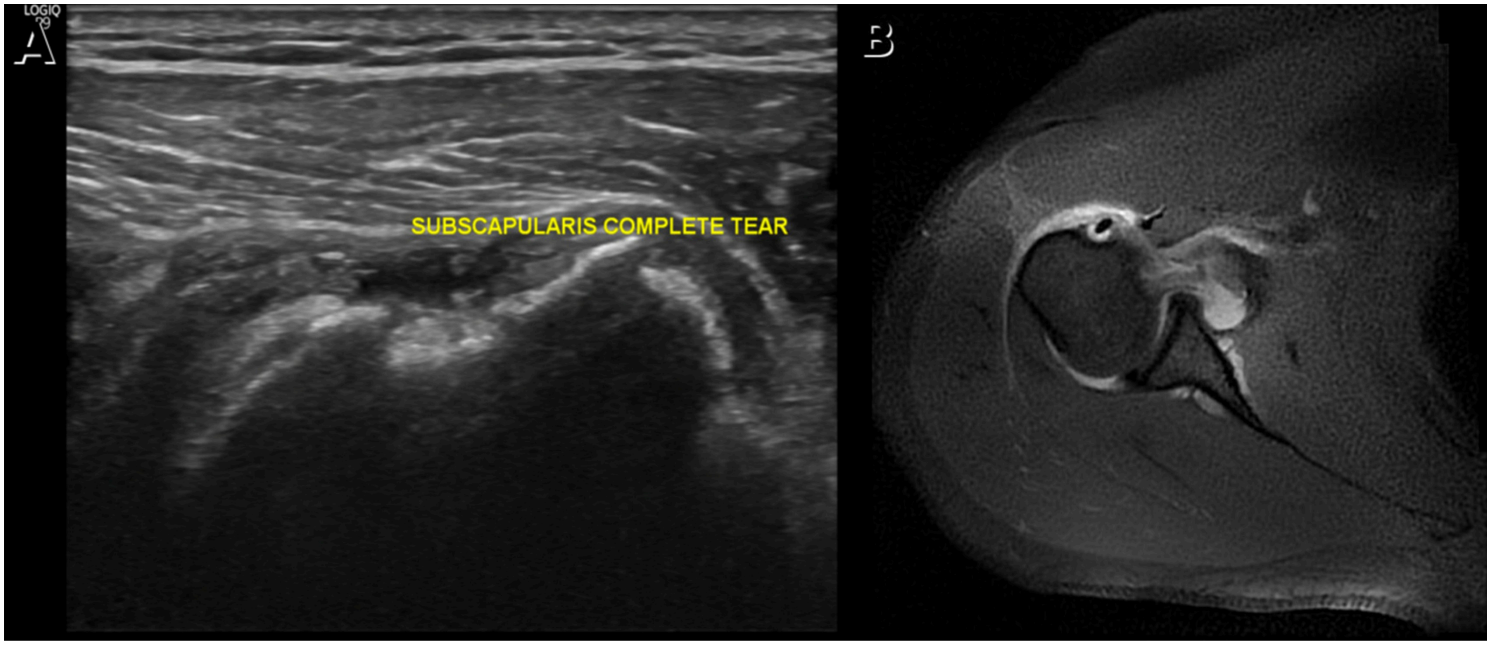


Figure 2

Full-thickness tear of subscapularis tendon on HRUSG and 3T MRI

A *High-resolution ultrasound image of the subscapularis tendon in longitudinal view demonstrating a complete (full-thickness) tear with tendon retraction (arrow).* **B** *Corresponding axial proton density fat-suppressed (PDFS) MR image confirming full-thickness tear of the subscapularis tendon with surrounding fluid and retraction of the torn tendon (arrow). HRUSG = high-resolution ultrasonography; PDFS = proton density fat suppressed.*

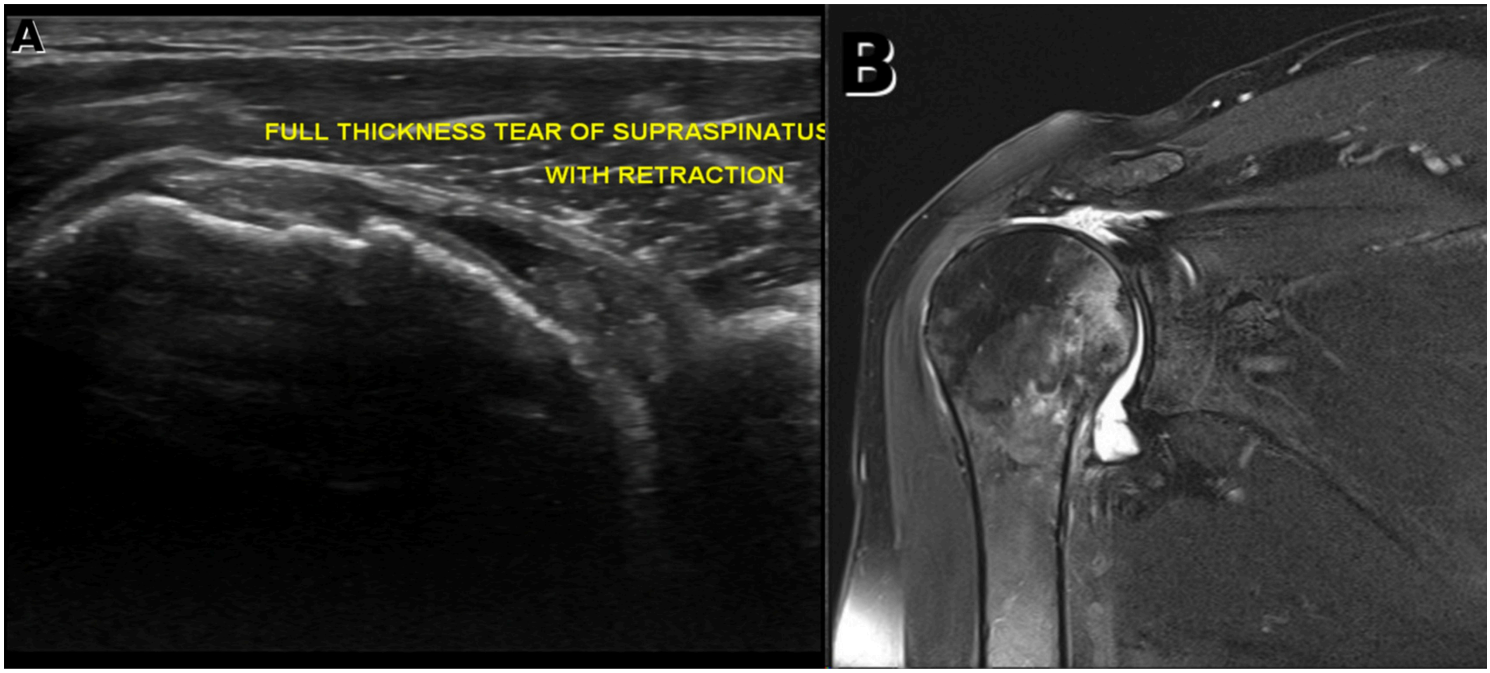


Figure 3

Full-thickness tear of supraspinatus tendon on HRUSG and 3T MRI.

A *Longitudinal HRUSG image showing a complete tear of the supraspinatus tendon with retraction of the torn end (arrow).* **B** *Sagittal PDFS MR image demonstrating full-thickness tear of the supraspinatus tendon with joint effusion and retraction of the torn part (arrow). PDFS = proton density fat suppressed.*

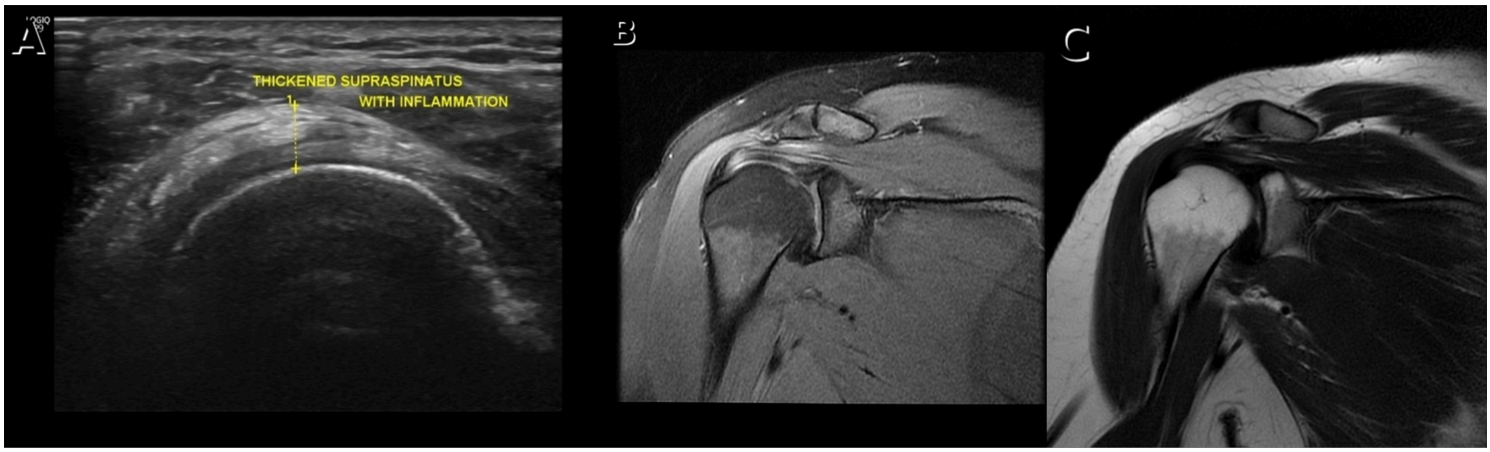
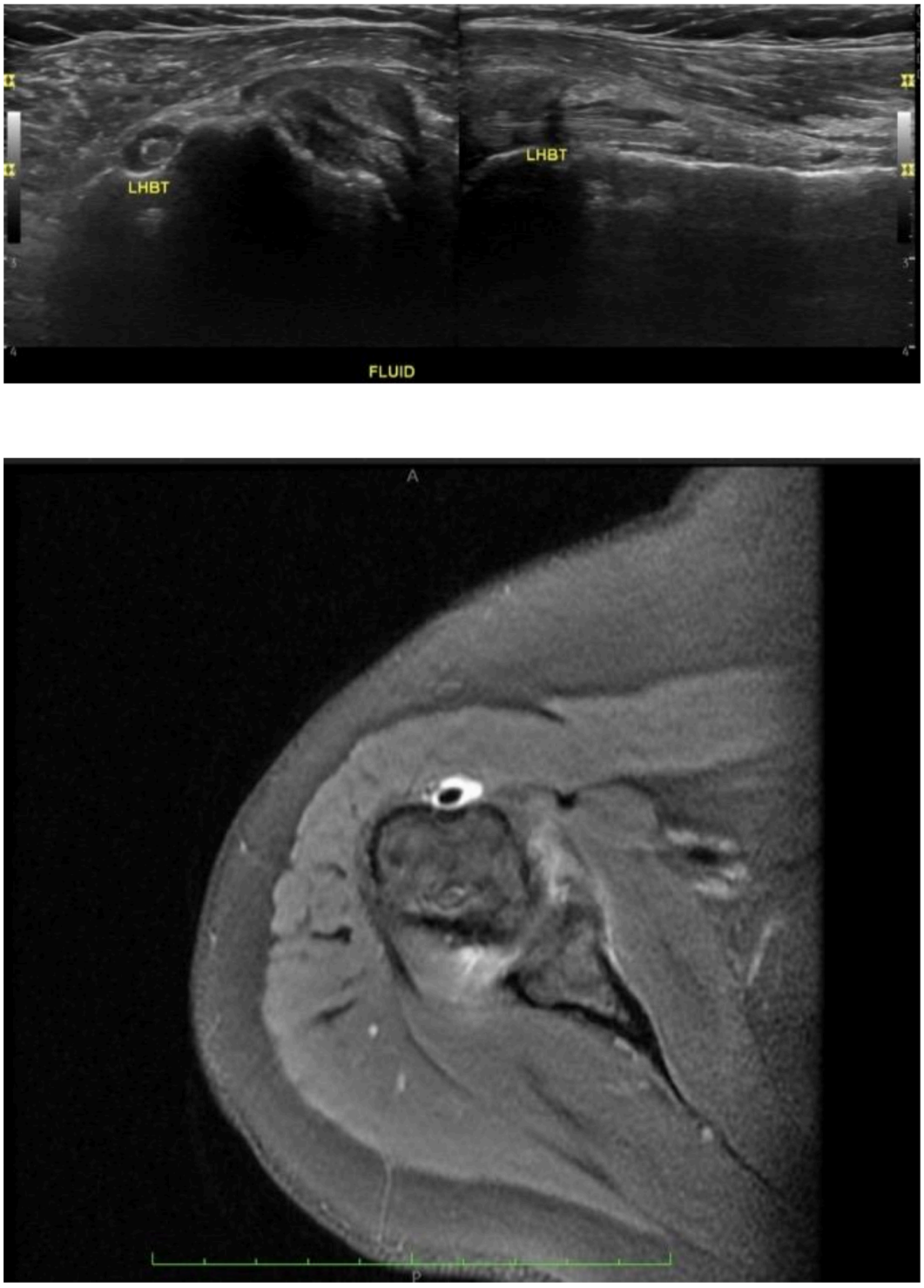


Figure 4

Tendinosis of supraspinatus tendon: HRUSG and 3T MRI correlation.

A *Longitudinal HRUSG image showing focal hypoechogenicity (arrow) with thickening of the supraspinatus tendon, consistent with tendinosis.* **B** *Coronal PDFS MR image demonstrating focal hyperintensity and thickening of the supraspinatus tendon.* **C** *Coronal T2-weighted MR image confirming focal hyperintensity and tendon thickening in keeping with tendinosis. The absence of fluid-equivalent T2 signal distinguishes this from a tear. PDFS = proton density fat suppressed.*

Fig. 5 Tendinosis of the long head of biceps tendon on HRUSG and 3T MRI.



A *HRUSG images of the long head of biceps tendon (LHBT) in axial and longitudinal views showing peritendinous fluid and synovial thickening (arrows). The tendon itself appears thickened.* **B** *Axial PDFS MR image demonstrating hyperintense peritendinous fluid around the LHBT in the bicipital groove (arrow), consistent with LHBT tendinosis. LHBT = long head of biceps tendon; PDFS = proton density fat suppressed.*

Figure 5

See image above for figure legend

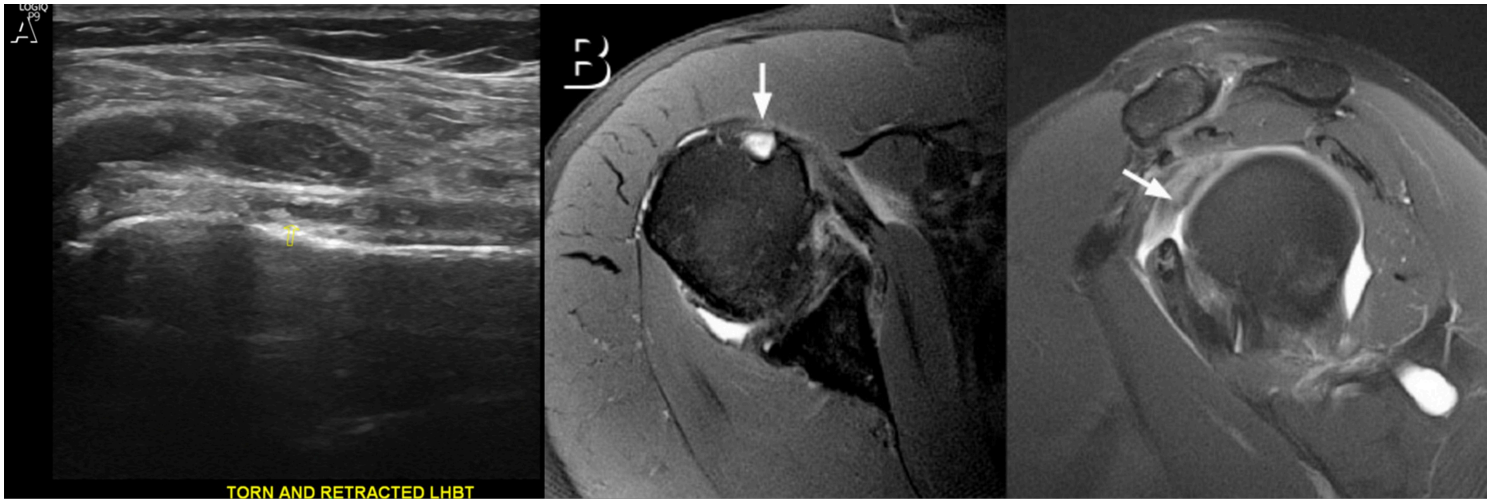


Figure 6

Complete tear of the long head of biceps tendon on HRUSG and 3T MRI.

A *Longitudinal HRUSG image demonstrating a completely torn and proximally retracted long head of biceps tendon (LHBT) with absence of the tendon in the bicipital groove (arrow).* **B** *Axial PDFS MR image confirming absence of the LHBT at the level of the bicipital groove (arrow) without evidence of subluxation or dislocation, indicating complete tear with proximal retraction. LHBT = long head of biceps tendon; PDFS = proton density fat suppressed.*

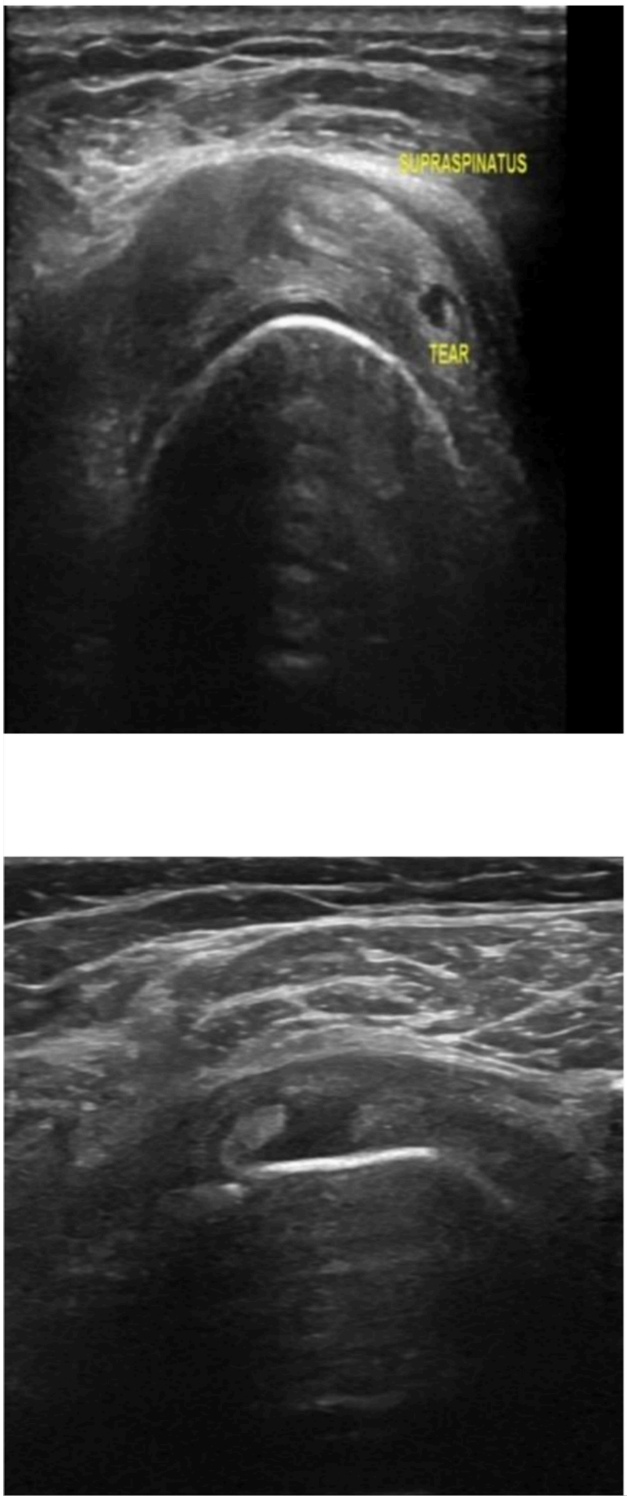


Fig. 7 Intrasubstance tear of supraspinatus tendon on HRUSG and 3T MRI.

A *Longitudinal HRUSG image of the supraspinatus tendon showing a focal hypoechoic defect confined within the substance of the tendon (arrow), not extending to either the articular or bursal surface.* **B** *Coronal PDFS MR image demonstrating a hyperintense focal defect (arrow) limited to the intratendinous portion of the supraspinatus tendon without bursal or articular surface involvement, consistent with an intrasubstance tear. PDFS = proton density fat suppressed.*

Figure 7

See image above for figure legend



Figure 8

Full-thickness tear of infraspinatus tendon on HRUSG and 3T MRI.

A *HRUSG image of the infraspinatus tendon demonstrating a full-thickness hypoechoic gap within the tendon fibres (arrow).* **B** *Axial PDFS MR image confirming full-thickness tear of the infraspinatus tendon with peritendinous fluid signal intensity (arrow). PDFS = proton density fat suppressed.*

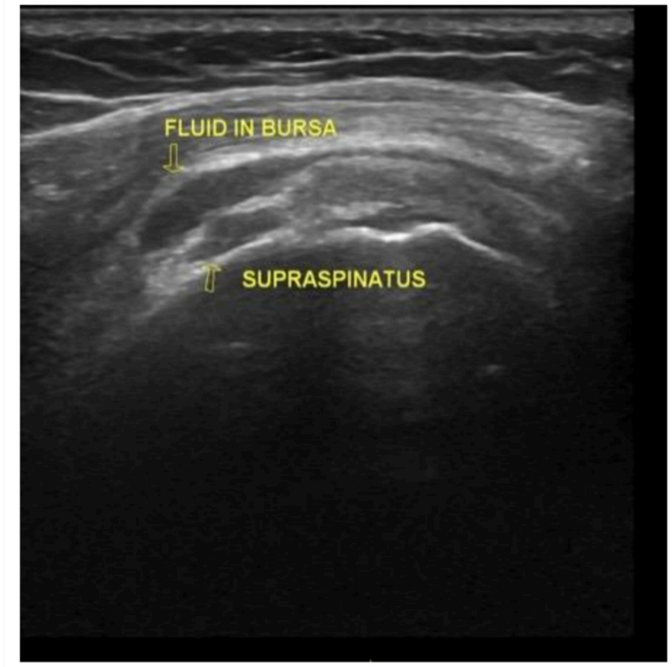




Fig. 9 Partial-thickness articular-surface tear of supraspinatus tendon on HRUSG and 3T MRI.

A *Longitudinal HRUSG image of the supraspinatus tendon showing a partial-thickness tear involving the articular-surface fibres (arrow). The bursal-surface fibres remain intact with no tendon retraction. Fluid is also noted in the subacromial–subdeltoid bursa.* **B** *Sagittal PDFS MR image demonstrating a hyperintense defect in the articular-surface fibres of the supraspinatus tendon (arrow) with fluid in the subacromial–subdeltoid bursa and no tendon retraction, confirming a partial-thickness articular-surface tear. PDFS = proton density fat suppressed; SASD = subacromial–subdeltoid.*

Figure 9

See image above for figure legend